File Copy 835

JOURNAL OF CATALYSIS 82, 382–394 (1983)

Importance of Catalyst Dispersion in the Gasification of Lignite Chars

LJUBISA R. RADOVIC, PHILIP L. WALKER, JR., AND ROBERT G. JENKINS

Department of Materials Science and Engineering, The Pennsylvania State University, University Park, Pennsylvania 16802

Received November 22, 1982; revised February 28, 1983

Lignite chars were prepared in N_2 under widely varying conditions of pyrolysis heating rate, temperature, and residence time. Their reactivities were measured by isothermal thermogravimetric analysis in 0.1 MPa air. A major decrease in char reactivity was observed with increasing severity of heat-treatment conditions. The relatively high gasification reactivity of lignite chars, compared to those obtained from higher rank coals, is due to the catalytic effect of the initially very highly dispersed CaO on the char surface. Char deactivation is caused primarily by CaO crystallite growth, measured by X-ray diffraction line broadening. When the reactivities of the various chars are expressed as turnover frequencies, i.e., per unit catalyst site, differences in observed rates of about 200 times are reduced to within 1 order of magnitude. Thus, it has been shown that the commonly observed and heretofore empirically treated lignite char deactivation with increasing severity of pyrolysis conditions can be correlated with a decrease in a measurable fundamental property of the chars: catalyst dispersion.

INTRODUCTION

In kinetic studies of coal gasification it is frequently assumed that the reactions occurring between the rapidly devolatilized char and the gases in contact with it fall into the category of gas–solid noncatalytic reactions (*1, 2*). In such studies the parameters which have the predominant effect on the reaction rate are taken to be the effective gas diffusivity in the pores and the total surface area of the reacting solid. Considerable efforts have been made in the past to measure or calculate the initial values of these parameters (for a review see, for example, Refs. (*3*) and (*4*)) and to predict or measure their changes in the course of char gasification reactions (*5–14*). In cases of good agreement between theory and experiment, it is often found that the proposed models contain many adjustable parameters that cannot be related easily to measurable physical properties of the char. More often than not, however, the experimentally observed differences in reactivity of carbons in general, including coal chars, cannot be satisfactorily explained when this approach is used (*15, 16*). This is not surprising when one realizes that it is too often ignored that the inorganic constituents, which are invariably present in coals, can act as more or less efficient gasification catalysts. For example, catalysis plays a major role in the reactivity of lignite chars (*17–21*). These can be visualized as supported catalysts, in which the char (carbon) acts as a support and the inorganic impurities (principally Ca species) act as the catalyst. The presence of exchangeable cations (mainly Ca^{2+}) associated with the carboxyl groups in the lignites makes possible their very high initial dispersion upon pyrolysis (*22, 23*). Therefore, lignite char gasification should be treated as a catalytic gas–solid reaction in which the catalyst dispersion has a major effect on the reaction rate. In previous studies of lignite char gasification (*17–21*), the catalyst has neither been clearly identified nor has its dispersion been measured.

0021-9517/83 $3.00

We have shown recently (*23*) that the relatively high gasification reactivity of lignites is due primarily to the catalytic effect of the highly dispersed CaO on the char surface. We have also correlated the process of char deactivation (achieved by increasing the pyrolysis residence time) with a decrease in CaO dispersion. This paper gives a more detailed and quantitative analysis of this correlation.

EXPERIMENTAL

Coal preparation. A previously well-characterized lignite from North Dakota (PSOC-246) was used in this study (*24, 25*). A size-graded fraction of the raw lignite (mean particle size ~ 170 μm) was washed with HCl and HF in order to remove essentially all the inorganic constituents. This demineralized coal (Demcoal) was subsequently ion-exchanged with Ca^{2+}, using a 1.5 *M* solution of Ca acetate. Ion exchange with Cu^{2+} was also carried out, using a 0.5 *M* solution of Cu acetate. Details of the experimental procedures are reported elsewhere (*22, 26*).

Coal pyrolysis. The demineralized and cation-exchanged lignite (Dem+Ca and Dem+Cu) was devolatilized in a stream of N_2 (99.99% purity) by both slow and rapid pyrolysis. The residence time was varied between 0.3 s and 1 h. The final pyrolysis temperature was between 975 and 1475°K. Slow pyrolysis (10°K/min) was performed in a conventional horizontal-tube furnace. Rapid pyrolysis (~10^4°K/s) was conducted in an entrained-flow furnace, described in detail elsewhere (*22, 27*).

Char reactivity measurements. Reactivities of the various chars were determined by isothermal thermogravimetric analysis (TGA) in 0.1 MPa air. The high reactivity of carbon in air (*17*) allowed operation at low temperatures, typically between 525 and 725°K. Under these conditions the concentration of active sites, created at higher temperatures (≥975°K), did not change significantly between the pyrolysis and gasification steps. Further details of the experimental procedure are given elsewhere (*22, 23, 26*).

Char characterization. The amounts of Ca and Cu added to the demineralized coal and retained in the chars after pyrolysis were determined by emission spectroscopy. X-Ray diffraction (XRD) patterns were obtained for selected samples in order to determine the chemical state and dispersion of the catalyst on their surface. A Rigaku diffractometer (Geigerflex D/max, 40 kV, 20 mA, Cu$K\alpha$ radiation) was used. In an attempt to obtain independent information about CaO dispersion, X-ray photoelectron spectroscopy (XPS) and selective chemisorption were also performed. A conventional volumetric apparatus was used for chemisorption (*4*). Adsorption isotherms were obtained with CO_2 at 298°K. After the first adsorption isotherm was obtained, the physically adsorbed gas was evacuated at 298°K for 3 h. Subsequently, a second adsorption isotherm was determined in the same relative pressure range.

RESULTS

The acid washing of the lignite is quite effective in removing essentially all of its inorganic constituents. The ash content was reduced from 9.7 to about 0.2 wt%. Ion exchange with Ca acetate resulted in a loading of about 2.9 wt% Ca, compared to 1.5 wt% in the raw coal.

Figure 1 shows the effect of pyrolysis temperature on the reactivity of Dem+Ca-char. The residence time in all cases was 1 h and the samples were devolatilized at 10 K/min. The plots of char conversion (burn-off) versus time were essentially linear up to about 40–50% burn-off and subsequently exhibited a gradual decrease in slope. In all cases, the maximum slope was used in the calculation of reported reactivities. The activation energy was about 130 kJ/mol, essentially identical to the value obtained for the gasification of demineralized char (*26*). Reactivities were independent of gas flow rate and sample bed depth. Thus, interparticle heat and mass transfer limitations

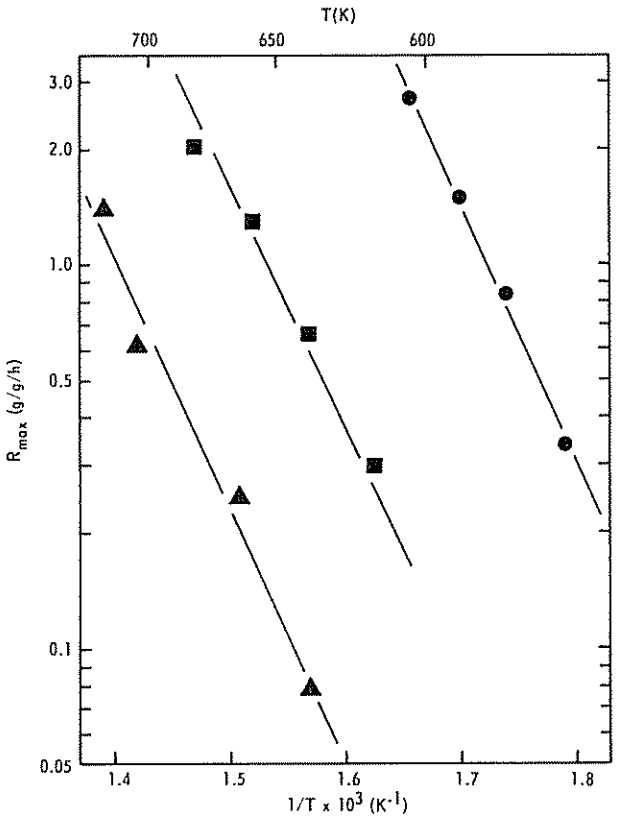

FIG. 1. Effect of pyrolysis temperature on the reactivity of Dem+Ca-char (slow pyrolysis; residence time, 1 h). ●, 975°K; ■, 1275°K; ▲, 1475°K.

were eliminated. There was also no effect on reactivity of a threefold variation in particle size, between 60 and 170 μm. This variation, however, probably did not affect appreciably the accessibility of the reactant gas to the micropores (<2 nm in size) where most of the char surface area resides. This criterion is thus not sufficient to show the absence of intraparticle mass transfer limitations. A complementary study was necessary to clarify this point. The results, reported in detail elsewhere (*26*), suggest that the observed reactivities are, indeed, intrinsic, chemically controlled rates. The absolute gasification rates were always kept below 5 mg/h in order to prevent ignition and nonisothermal behavior (*22*, *23*).

Figure 2 gives the XRD patterns obtained for the starting Dem+Ca-coal and the chars whose reactivities are shown in Fig. 1. As discussed previously (*23*), it is clearly seen in Figs. 2c and d that CaO is the predominant Ca species which catalyzes lignite char gasification.

Table 1 summarizes the information on reactivities and CaO dispersion for a series of Dem+Ca-chars with widely varying pyrolysis temperature–time histories. The sample code (column 1) denotes the mode of pyrolysis (R = rapid, S = slow) and the residence time at pyrolysis temperature. Unless otherwise indicated in parentheses, all samples were prepared at 1275°K. It is seen in column 2 that the CaO content of the rapidly devolatilized chars varies from 8.0 to 10.4%. This variation parallels the increase in the C/H ratio of the char with increasing pyrolysis residence time (*23*). In the case of slowly devolatilized samples, the CaO content is consistently lower. This

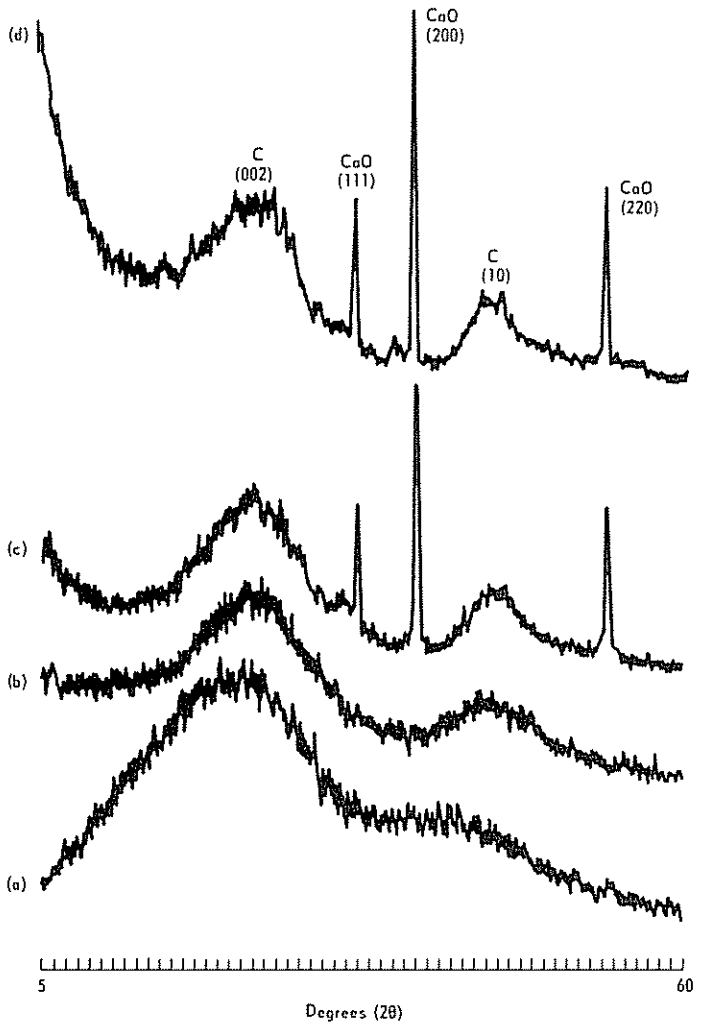

FIG. 2. X-Ray diffraction patterns for Dem+Ca-coal and chars (slow pyrolysis; residence time, 1 h). (a) coal, (b) 975°K, (c) 1275°K, (d) 1475°K.

is a reflection of the lesser extent of volatilization of carbon-containing gases in fixed-bed pyrolysis, compared to entrained-flow pyrolysis, due to enhanced secondary char-forming reactions (*28, 29*). The very low CaO content of the char obtained at 1475°K (5.6%) suggests that some Ca may also be lost by volatilization. Indeed, from the experimentally measured weight loss of about 45% for this char, one would expect a CaO content of about 7.4%, based on the 2.9% Ca content in the starting coal.

The average crystallite diameter (D) of CaO (column 3, Table 1) was calculated using the line broadening concept and the Scherrer equation (*30*) in the form:

$$D = \frac{K\lambda}{(B^2 - b^2)^{1/2}(\cos\theta)}. \qquad (1)$$

In Eq. (1), λ is the wavelength of the x-rays and θ is the diffraction angle. The instrumental broadening (b) was determined to be 0.175° (2θ) from the (111) reflection of Si crystals (>10 μm). The (200) CaO peak widths at half height (B) were determined from scans made at 0.5° (2θ) min^{-1}. The

TABLE 1

Effect of Pyrolysis Conditions on the Reactivity of Dem+Ca-Char and CaO Dispersion

Sample	CaO (wt%)	D (nm)	d (%)	S_{CaO} (m^2/g CaO)	R_{625} (g/g C/h)	R_{625} (g/m^2 CaO/h)	TOF (s^{-1})
R − 0.3 s	8.0	—[a]	>25[b]	>300	~10[c]	<0.42 (≥0.10)	<0.67 (≥0.16)
R − 1.8 s	9.3	—[a]	>25[b]	>300	~10[c]	<0.36 (≥0.09)	<0.58 (≥0.14)
R − 30 s	9.5	21.5	5.8	72	1.3	0.19	0.30
R − 1 min	9.5	23.5	5.3	65	1.1	0.18	0.29
R − 3 min	8.9	23.5	5.3	65	1.1	0.19	0.30
R − 5 min	10.4	24.5	5.1	63	1.0	0.15	0.24
S − 0 h	7.6	25.0	5.0	62	0.90	0.19	0.30
S − 1 h	7.5	28.0	4.4	55	0.40	0.10	0.16
S − 1 h (975°K)	7.2	—[a]	>25[b]	>300	~5.0[c]	<0.23 (≥0.03)	<0.37 (≥0.05)
S − 1 h (1475°K)	5.6	47.0	2.6	33	0.05	0.03	0.05

[a] Not detectable by XRD.
[b] Assuming $D < 5$ nm.
[c] Extrapolated value.

commonly used value of the Scherrer constant ($K = 0.9$) was used in all calculations. Column 4 gives the values of dispersion (percentage exposed) of CaO, calculated using:

$$d_{CaO} = \frac{5M}{D\rho A N_A} = \frac{1.24}{D} \qquad (D \text{ in nm}). \quad (2)$$

In Eq. (2) M is the molecular weight, ρ is the density, A is the surface area occupied by one CaO molecule, and N_A is Avogadro's number. It is assumed that CaO crystallites are regular cubes with five faces exposed and accessible to the reactant gas, with each molecule occupying 0.115 nm^2. Column 5 gives the values of dispersion of CaO in terms of surface area, using:

$$S_{CaO} = \frac{5}{D\rho} = \frac{1538}{D} \qquad (D \text{ in nm}). \quad (3)$$

Column 6 gives the values of reactivity of the different chars at 625°K, expressed per unit initial mass of dry ash-free char. Column 7 gives the reactivity values expressed per unit catalyst surface area. Column 8 gives the turnover frequencies (TOF) in atoms of carbon gasified per surface molecule of CaO per second.

Figure 3 shows the effect of pyrolysis conditions on the reactivity of Dem+Cu-char. The activation energy in all cases was again about 130 kJ/mol.

Figure 4 shows the XRD patterns for Dem+Ca- and Dem+Cu-chars, both prepared by rapid pyrolysis at 1275°K for 0.3 s. It is seen that the crystallite size of the Cu

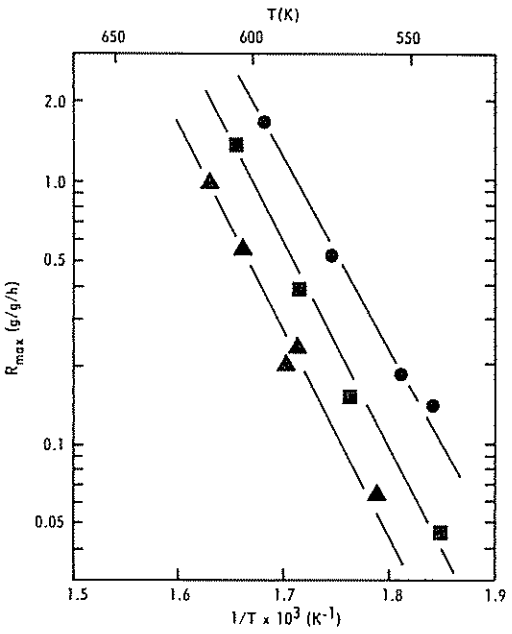

FIG. 3. Effect of pyrolysis conditions on the reactivity of Dem+Cu-char. ●, R − 0.3 s (1275°K); ■, S − 1 h (975°K); ▲, S − 1 h (1275°K).

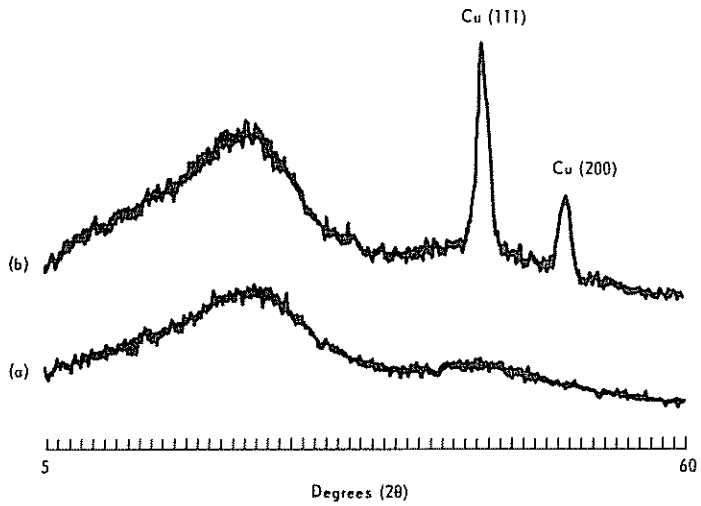

FIG. 4. X-Ray diffraction patterns for short-residence-time Dem+Ca- and Dem+Cu-chars (pyrolysis temperature, 1275°K; residence time, 0.3 s). (a) Dem+Ca, (b) Dem+Cu.

species is already large enough to be detected by XRD. On the other hand, CaO crystallites formed under these conditions are too small to be detected (*23*). Also, it is seen that, in contrast to the Ca-exchanged lignite, the decomposition of the Cu-exchanged carboxyl groups leads to the formation of metallic Cu.

Average crystallite sizes of Cu on the various chars are given in Table 2, together with their respective reactivities and Cu-dispersion values, calculated as in Table 1. The appropriate equations are: $d_{Cu} = 1.04/D$ and $S_{Cu} = 558/D$ (D in nm).

DISCUSSION

We have shown recently (*23*) that the Dem+Ca-chars exhibit essentially the same gasification behavior as the raw (as-received) lignite chars. Thus, they are convenient "model compounds" for studying the effect of catalysis in lignite char gasification at a fundamental level, in the absence of complicating (and obscuring) effects of other inorganic constituents. It was also shown that the Dem+Ca-chars are about 50 times more reactive than the Dem-chars obtained under identical pyrolysis conditions (*23*). Clearly, Ca is a very efficient carbon gasification catalyst. Indeed, Walker *et al.* (*31*) conclude that it is the most important *in situ* catalyst for the gasification of American coal chars in O_2, CO_2, and H_2O.

Importance of Catalyst Dispersion

Results presented in Fig. 1 and elsewhere (*23*) show that the increase in severity of

TABLE 2

Effect of Pyrolysis Conditions on the Reactivity of Dem+Cu-Char and Cu Dispersion

Sample	Cu (wt%)	D (nm)	d (%)	S_{Cu} (m^2/g Cu)	R_{600} (g/g C/h)	R_{600} (g/m^2 Cu/h)	TOF (s^{-1})
R − 0.3 s (1275°K)	2.2	10.0	9.0[a]	56	2.3	1.9	1.7
S − 1 h (975°K)	1.4	17.0	5.3	33	1.0	2.2	2.0
S − 1 h (1275°K)	1.4	20.0	4.5	28	0.46	1.2	1.1

[a] $A = 0.065$ nm²/atom Cu.

lignite pyrolysis conditions causes a major decrease in the gasification reactivity of the remaining char. The obvious question, which nevertheless has not been adequately addressed, is: what is (are) the reason(s) for the observed char deactivation? In previous work, we have shown, both in the case of demineralized (*26*) and raw (*32*) chars, that the total surface area is not a relevant parameter. That is, two chars having the same total surface area, measured using CO_2 adsorption at 298°K and the Dubinin–Polanyi approach (*4*), can have widely differing gasification reactivities.

Figure 2 provides, qualitatively, one answer to the above question. It is seen, at one extreme, that in the char pyrolyzed at a relatively low temperature of 975°K, Ca species are not detectable by XRD and are thus very well dispersed. This is not surprising, since ion exchange initially provides essentially atomic dispersion, i.e., one Ca^{2+} per two carboxyl groups in the lignite. During pyrolysis, the carboxyl groups decompose at an early stage and CO_2 is evolved. Depending upon the temperature and residence time, the Ca species gain more or less mobility on the surface and crystallite growth becomes possible. Thus, at the other extreme, Figs. 2c and d clearly show that at 1275°K and above relatively large crystallites of CaO are formed, with significantly poorer dispersion.

A quantitative analysis of the decrease in CaO dispersion and its effect on char reactivity is given in Table 1. For the short-residence-time (0.3–1.8 s) and low-temperature (975°K) chars, a crystallite size of <5 nm is arbitrarily assumed (column 3). This is the usually cited lower XRD detection limit for supported metal catalysts. It is interesting to note that even at temperatures below the Tammann point (*33*, *34*) of CaO (1490°K), in this case at 1275°K, crystallite growth (sintering) is very rapid, the dispersion decreasing by a factor of at least four in the first 30 s. Further decrease in catalyst dispersion with increasing residence time between 30 s and 1 h is relatively small. When the pyrolysis temperature is increased to 1475°K, i.e., close to the Tammann temperature, at which significant particle mobility is expected, an additional almost twofold decrease in dispersion is observed.

Column 6 of Table 1 shows that when the reactivities of the various chars are normalized with respect to the initial char weight, they differ by as much as 200 times. On the other hand, when they are normalized with respect to the CaO surface area (column 7) or when the rates are expressed as turnover frequencies (column 8), these differences are reduced to within 1 order of magnitude. The upper limit of turnover frequencies for the short-residence-time and low-temperature chars was set by assuming the mean CaO crystallite size to be <5 nm. The lower limit can be set by realizing that S_{CaO} (column 5) cannot be higher than 1240 m^2/g. This value (100% dispersion) is obtained if it is assumed that each CaO molecule is a surface molecule. Thus, the corresponding lower limits are indicated in parentheses in columns 7 and 8 of Table 1.

It is clear from the preceding discussion that the gasification reactivity of lignite chars is dominated by the concentration of catalyst (CaO) active sites. The fact that there is still a sixfold difference in turnover frequencies that needs explanation suggests two possibilities: (a) the concentration of carbon-active sites is also important in the kinetics of catalyzed gasification, and/or (b) the average crystallite size obtained from XRD line broadening does not give exactly the true value of catalyst dispersion.

The first possibility is discussed at length in a companion publication (*26*). There it is shown (in the case of demineralized lignite chars, where the uncatalyzed gasification is expected to be dominant) that the oxygen chemisorption capacity of the various chars (at 375°K and 0.1 MPa air) decreases by a factor of about 10 with increasing severity of pyrolysis, in the same temperature–time range as used here. Also, the average carbon crystallite diameter of the chars in-

creases from about 2.2 to about 3.5 nm, measured from the line broadening of the (*10*) carbon peak. It was assumed that these are valid indicators of the concentration of carbon-active sites, at least from a relative standpoint.

With respect to the second possibility, one must be aware of all the assumptions involved in the determination of catalyst dispersion from XRD line broadening. If a wide particle size distribution exists, the amount of "x-ray amorphous" material (*35*) may vary from sample to sample, thus affecting the dispersion values. The existence of polycrystalline CaO particles is also probable. However, no attempt has been made in the present study to test the validity of the assumptions made in Table I in going from column 3 to column 7. It should be noted that the low TOF values in column 8 are obtained precisely for those chars that are expected to have a lower concentration of carbon active sites, i.e., for the more severely heat-treated chars. In these chars the CaO particles are also expected to be less porous, the CaO crystallite boundaries are expected to be less accessible to the reactant gas and the estimated surface areas in Table I are probably too high. Having in mind the very small contribution of carbon-active sites to the overall gasification reactivity of Dem+Ca-chars (*23*), it is concluded from the above discussion that probable errors, within 1 order of magnitude, in the estimation of catalyst dispersion by XRD are responsible for the observed (relatively small) differences in the TOF values in Table I. The reported values should be considered, therefore, as the lower limits of turnover frequency.

Considerable effort has been made in the course of this study to verify the CaO dispersion data obtained by XRD. In preliminary XPS studies, two Dem+Ca-chars at the opposite ends of the pyrolysis time scale were analyzed: R − 0.3 s and S − 1 h, both prepared at 1275°K. It was expected that the Ca/C atomic ratio would be higher for the former char, since CaO is more highly dispersed on its surface. However, the opposite result was obtained; the Ca/C ratio was higher for the more severely heat-treated chars. It was concluded that with the increase in the severity of pyrolysis conditions, the CaO particles tend to diffuse out of the micropores toward the outer surface of the char in order to facilitate sintering, resulting in surface enrichment. The same observation was made recently by Wigmans *et al.* in the case of Ni dispersed on a microporous activated carbon (*36*). Being a surface technique, with the escape depth of electrons of less than 5 nm, it is probable that XPS "sees" only these large CaO crystallites on the outer surface of char particles (ground to ~10 μm). Thus it cannot be used to determine catalyst dispersion. The scanning electron micrographs shown in Fig. 5 provide evidence for the validity of this conclusion. Calcium-containing species were identified by x-ray energy spectroscopy on the surface of both samples. However, the Ca peaks were much more intense in the case of char S − 1 h. The particles of CaO, previously identified by XRD (see Fig. 2c), are clearly seen (Fig. 5a) in abundance on the surface of this char. On the other hand, they are not visible on the surface of char R − 0.3 s (Fig. 5b). These results also suggest that CaO is much better dispersed on the surface of chars which have undergone milder heat treatment.

The choice of adsorbate for determining catalyst dispersion by selective chemisorption is not a straightforward matter in the case of the CaO/lignite char system. It is well known that CO_2 readily chemisorbs on the oxides of alkali and alkaline-earth metals (*37–40*). Its use was also attempted in our work. A typical set of adsorption isotherms at 298°K is given in Fig. 6. The difference in volume adsorbed between the two isotherms at an arbitrarily selected relative pressure is attributed to CO_2 chemisorbed on CaO. A sample with one of the highest dispersions of Ca (≳25%) was used:

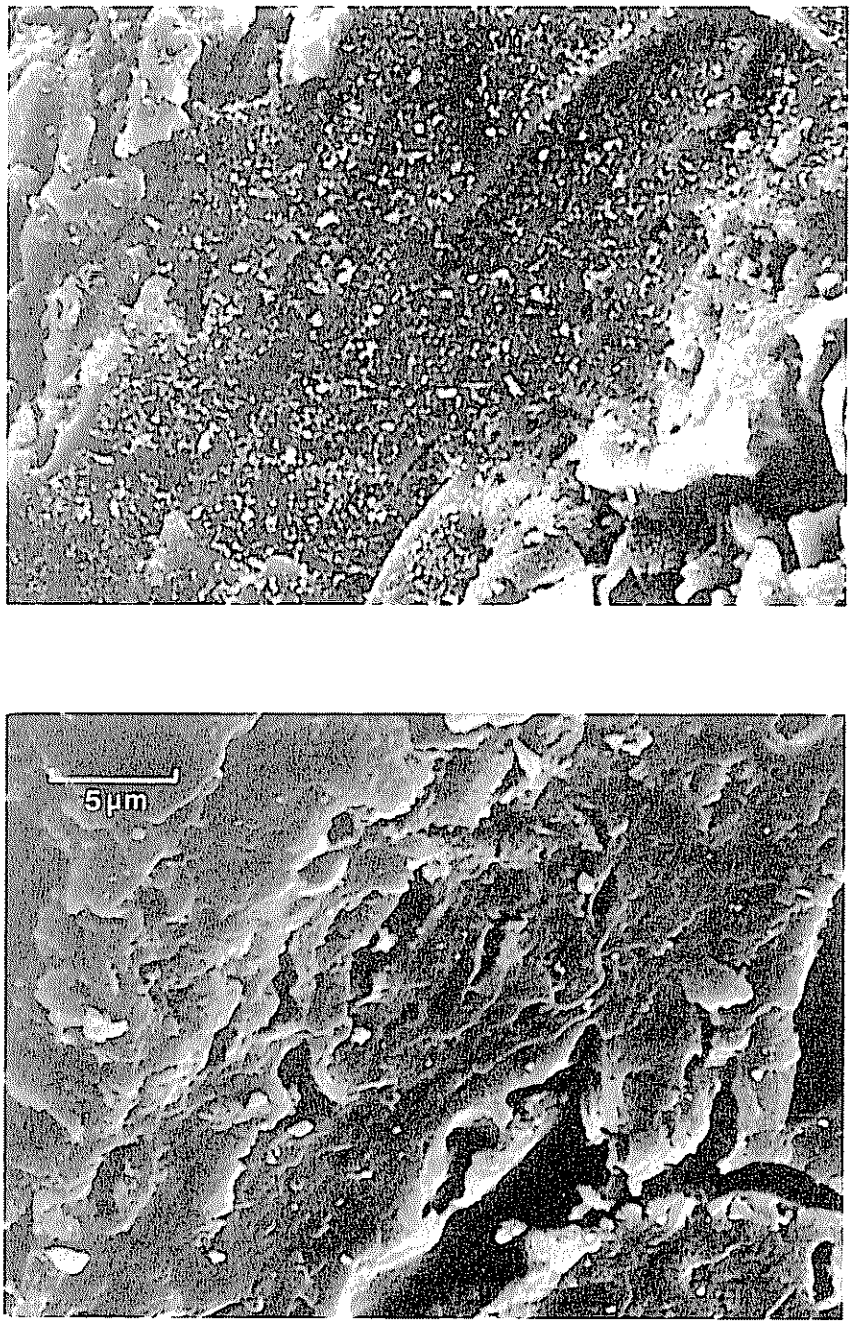

FIG. 5. Scanning electron micrographs of Dem+Ca-chars: (a) S − 1 h (1275°K), (b) R − 0.3 s (1275°K).

R − 1.8 s, prepared at 1275°K. One complicating factor is immediately apparent from Fig. 6: the amount of physically adsorbed CO_2 on the highly porous char (support) is very large, about 30 cm^3 (STP)/g at 4 kPa CO_2. The reproducibility limits for physical adsorption were determined on Dem-chars and found to be ±1 cm^3 (STP)/g. Thus, only when the amount of CO_2 chemisorbed on CaO exceeds about 2 cm^3/g can the disper-

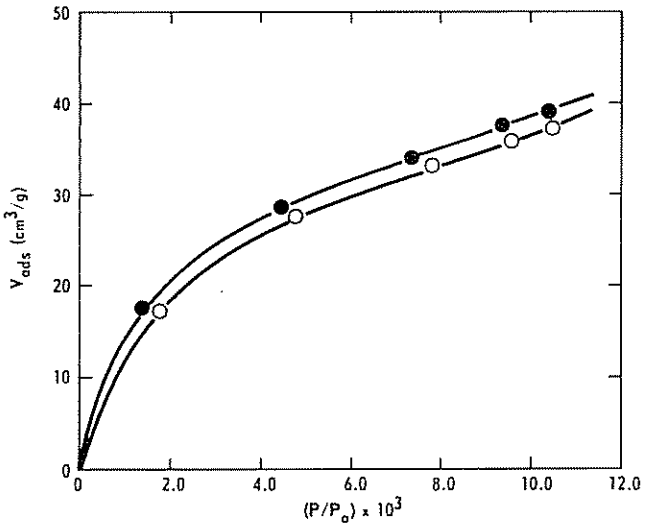

FIG. 6. Adsorption isotherms at 298°K for CO_2 on Dem+Ca-char R = 1.8 s (1275°K). Initial outgassing temperature, 385°K. Intermediate outgassing temperature, 298°K. ●, First isotherm; ○, second isotherm.

sion be reliably measured. In the case of severely heat-treated chars, where the mean CaO particle size is at least 20 nm (see Table 1), an order-of-magnitude calculation readily shows that this condition is not fulfilled. However, in the case of sample R = 1.8 s shown in Fig. 6, a higher volume of CO_2 chemisorbed was expected, at least 4–5 cm^3/g, instead of the experimentally observed ~2 cm^3/g. Obviously, some of the CaO surface is not accessible to CO_2 molecules at 298°K. This conclusion is discussed in more detail and substantiated elsewhere (*22*).

It was shown by XPS (*23*) that CaO particles are indeed present on the surface of the short-residence-time chars even though they are not detectable by XRD. It was reasoned on the basis of these results that, if a catalyst with a much lower Tammann temperature is prepared under the same conditions, it would be detected by XRD, due to its easier (faster) sintering. Indeed, this is shown to be the case in Fig. 4 for the Cu/char system. The mean crystallite size of Cu (Tammann point, 680°K) was calculated to be about 10 nm. By varying the heat-treatment conditions, Dem+Cu-chars of different reactivity were obtained (Fig. 3) and the correlation between char reactivity and catalyst dispersion was again tested. The results are shown in Table 2. Reactivities per unit mass of char (column 6) differ by a factor of 5. The turnover frequencies (column 8) differ by less than a factor of 2. Again, as in Table 1, the lower value of TOF is observed for the more severely heat-treated char. The significance of these results lies in the fact that in many cases of supported-metal catalysis, a good qualitative agreement has been found between metal dispersion measurements by XRD and other techniques (see, for example, Refs. (*41*) and (*42*)). Comparison of turnover frequencies in Tables 1 and 2 indicates that Cu is a better catalyst for char gasification in air than is CaO.

Mechanism of Catalysis

The mechanisms of catalysis of carbon gasification in general (*43–52*) and of CaO catalysis of char gasification in particular (*21, 44, 53*) are debatable issues that still need much investigation. For reactions in oxidizing atmospheres (O_2, CO_2, H_2O) catalyzed by alkali and alkaline-earth metals,

the oxygen-transfer mechanism is favored (*44*). The various pieces of circumstantial evidence obtained in this study and available in the literature, discussed below, suggest the following oxidation–reduction (redox) sequence:

$$C_e + CaO + O_2 \rightarrow CaO_2 + C_e\text{–}O\ (ads) \quad (4a)$$

$$C_b + CaO + O_2 \rightarrow CaO_2 + C_b\text{–}O\ (ads) \quad (4b)$$

$$2C_e + O_2 \rightarrow 2C_e\text{–}O\ (ads) \quad (4c)$$

$$C_b\text{–}O\ (ads) \rightarrow C_e\text{–}O\ (ads) \quad (4d)$$

$$C_e\text{–}O\ (ads) \rightarrow CO(g) \quad (4e)$$

$$2C_e\text{–}O\ (ads) \rightarrow CO_2(g) + C_e \quad (4f)$$

$$CaO_2 + C_b \rightarrow CaO + C_b\text{–}O\ (ads) \quad (4g)$$

$$CaO_2 + C_e \rightarrow CaO + C_e\text{–}O\ (ads) \quad (4h)$$

The proposed mechanism reflects the experimental finding that the concentration of both catalyst and carbon-active sites may influence the overall char gasification reactivity. It also provides independent, parallel paths for the uncatalyzed and catalyzed reactions.

Steps (4a–4c) represent the catalyst oxidation and the dissociative chemisorption of O_2 either on a catalyst or carbon active site. Two types of carbon sites are postulated: C_e denotes an active-carbon site located at the edge of the carbon crystallite, either free or at the catalyst–carbon interface; C_b denotes a basal (inactive) carbon atom at the catalyst–carbon interface. The formation of a higher surface oxide of Ca (either superoxide or peroxide) has been postulated, and in some cases demonstrated, in the literature. For example, Carberry *et al.* (*54*) suggested that the enhanced selectivity in Ag-catalyzed ethylene oxidation to ethylene oxide in the presence of a CaO promoter is due to superoxide formation on the surface of Ca sites as well as on the Ag sites. Among the alkaline-earth metals, the ease of formation of a higher oxide (related to the size of the cation) is: Mg < Ca < Ba. Both Ca and Ba are excellent gasification catalysts; Mg is a poor catalyst. This may well be due to its inability to undergo the redox cycle suggested above. In experiments described in detail elsewhere (*22, 26*), we have also shown that CaO is an excellent O_2 dissociation catalyst. No molecular O_2 was detected upon desorption to 1225°K. In the presence of CaO, the oxygen chemisorption capacity of a lignite char (R − 0.3 s) at 375°K increases by about 100%.

Step 4d represents the surface diffusion of oxygen from a basal carbon atom at the catalyst–carbon interface to an active carbon site. It has been shown recently (*55*) that CaO is also a very active catalyst for oxygen exchange in CO_2, i.e., for the scission of a C–O bond. This finding suggests the possibility of a spillover mechanism (*56*), indicated in steps, (4b,d,e,f).

Steps (4e,f) reflect the experimental fact that both CO and CO_2 are primary reaction products (*57*); only one of the possible ways of CO_2 formation is shown. Steps (4g,h) represent the catalyst reduction by carbon, i.e., the completion of the redox cycle.

The experimental fact that the same activation energy, of about 130 kJ/mol, was observed in the case of Dem-, Dem+Ca-, and Dem+Cu-chars also supports the suggested oxygen-transfer mechanism of catalysis, in which the role of the catalyst is to increase

the number of active sites, i.e., the preexponential term in the Arrhenius rate expression. However, the possible existence of a compensation effect (*58*) does not permit any additional mechanistic interpretation of this finding.

SUMMARY AND CONCLUSIONS

Lignite char gasification should be treated as a catalytic gas–solid reaction in which CaO acts as a very efficient *in situ* catalyst. Thus, a fundamental understanding of char gasification kinetics requires the knowledge of turnover frequencies, i.e., rates per unit catalyst site. The results presented in this paper have provided, for the first time to the knowledge of the authors, at least a semiquantitative correlation between char reactivity and catalyst dispersion. Further work in this direction is necessary to verify the dispersion data (obtained by x-ray diffraction) using a different, independent technique. X-Ray photoelectron spectroscopy and selective chemisorption of CO_2 were found not to be suitable techniques for the char/CaO system. Changes in catalyst dispersion and active-site concentration during reaction should also be investigated in order to explain the entire range of observed conversion versus reaction time curves.

An oxygen-transfer mechanism of catalysis of char oxidation is proposed. Calcium oxide is oxidized to a higher oxide and the higher oxide is reduced by carbon back to the lower oxide. Dissociative chemisorption of oxygen occurs both on the catalyst and carbon-active sites. Oxygen spills over from the catalyst–carbon interface and diffuses to a carbon-active site where gasification takes place.

ACKNOWLEDGMENTS

This study was supported by the Gas Research Institute, under Contract 5014-363-0235. Initial support for LRR in the form of a Fulbright Scholarship was provided by the Yugoslav-American Commission for Educational Exchange. The assistance of Dr. Katarzyna Steczko in the preparation of samples is gratefully acknowledged. Thanks are also due to Dr. L. Schmitt, of American Cyanamid, for the XPS work. The elemental analyses were performed by the staff of the Mineral Constitution Laboratory of The Pennsylvania State University. The coal samples were obtained from the Coal Research Section of The Pennsylvania State University.

REFERENCES

1. Szekely, J., Evans, J. W., and Sohn, H. Y., *in* "Gas–Solid Reactions," p. 108. Academic Press, New York, 1976.
2. Smith, J. M., *in* "Chemical Engineering Kinetics," Third ed., p. 636. McGraw–Hill, New York, 1981.
3. Walker, P. L., Jr., and Mahajan, O. P., *in* "Analytical Methods for Coal and Coal Products" (C. Karr, Ed.), Vol. I, p. 163. Academic Press, New York, 1978.
4. Mahajan, O. P., and Walker, P. L., Jr., ibid. p. 125.
5. Petersen, E. E., *AIChE J.* **3**, 443 (1957).
6. Hashimoto, K., and Silveston, P. L., *AIChE J.* **19**, 259 (1973); **19**, 268 (1973).
7. Simons, G. A., and Finson, M. L., *Combust. Sci. Technol.* **19**, 217 (1979).
8. Simons, G. A., *Combust. Sci. Technol.* **19**, 227 (1979).
9. Gavalas, G. R., *AIChE J.* **26**, 577 (1980).
10. Bhatia, S. K., and Perlmutter, D. D., *AIChE J.* **26**, 379 (1980).
11. Srinivas, B., and Amundson, N. R., *AIChE J.* **26**, 487 (1980).
12. Gavalas, G. R., *Combust. Sci. Technol.* **24**, 197 (1981).
13. Zygourakis, K., Arri, L., and Amundson, N. R., *Ind. Eng. Chem. Fundam.* **21**, 1 (1982).
14. Debelak, K. A., Clark, M. A., and Malito, J. T., *Amer. Chem. Soc. Prepr. Fuel Chem. Div.* **27**(1), 31 (1982).
15. Smith, I. W., *Fuel* **57**, 409 (1978).
16. Simons, G. A., *Carbon* **20**, 117 (1982).
17. Jenkins, R. G., Nandi, S. P., and Walker, P. L., Jr., *Fuel* **52**, 288 (1973).
18. Hippo, E. J., Jenkins, R. G., and Walker, P. L., Jr., *Fuel* **58**, 338 (1979).
19. Otto, K., Bartosiewicz, L., and Shelef, M., *Fuel* **58**, 85 (1979); **58**, 565 (1979).
20. Nandi, S. P., and Johnson, J. L., *Amer. Chem. Soc. Prepr. Fuel Chem. Div.* **24**(3), 17 (1979).
21. Sears, J. T., Muralidhara, H. S., and Wen, C. Y., *Ind. Eng. Chem. Process Des. Dev.* **19**, 358 (1980).
22. Radovic, L. R., "Importance of Catalysis and Carbon Active Sites in Lignite Char Gasification," Ph.D. thesis, The Pennsylvania State University, 1982.
23. Radovic, L. R., Walker, P. L., Jr., and Jenkins, R. G., *in* "Proceedings, International Symposium Fundamentals of Catalytic Coal and Carbon Gasification," p. 198. Amsterdam, September 1982.

24. Penn State/DOE Coal Data Base (PSOC-246), Coal Research Section, The Pennsylvania State University.
25. Morgan, M. E., Jenkins, R. G., and Walker, P. L., Jr., *Fuel* **60,** 189 (1981).
26. Radovic, L. R., Walker, P. L., Jr., and Jenkins, R. G., *Fuel,* in press.
27. Scaroni, A. W., Walker, P. L., Jr., and Essenhigh, R. H., *Fuel* **60,** 71 (1981).
28. Scaroni, A. W., Walker, P. L., Jr., and Jenkins, R. G., *Fuel* **60,** 558 (1981).
29. Gray, D., Cogoli, J. G., and Essenhigh, R. H., *in* "Coal Gasification," Advances in Chemistry Series, No. 131 (L. G. Massey, Ed.), p. 72. ACS, Washington, D.C., 1974.
30. Klug, H. P., and Alexander, L. E., *in* "X-Ray Diffraction Procedures," p. 687. Second ed. Wiley, New York, 1974.
31. Walker, P. L., Jr., Matsumoto, S., Hanzawa, T., Miura, T., and Ismail, I. M. K., *in* Proceedings, International Symposium "Fundamentals of Catalytic Coal and Carbon Gasification," p. 11. Amsterdam, September 1982.
32. Radovic, L. R., Walker, P. L., Jr., and Jenkins, R. G., *Fuel,* in press.
33. Baker, R. T. K., *Catal. Rev.-Sci. Eng.* **19,** 161 (1979).
34. Baker, R. T. K., *J. Catal.*, **78,** 473 (1982).
35. Pope, D., Smith, W. L., Eastlake, M. J., and Moss, R. L., *J. Catal.* **22,** 72 (1971).
36. Wigmans, T., Auwerda, K., Geus, J. W., and Moulijn, J. A., *in* "Extended Abstracts, 15th Biennial Conference on Carbon, Philadelphia, 1981," p. 441.
37. Emmett, P. H., and Brunauer, S., *J. Amer. Chem. Soc.* **59,** 310 (1937).
38. Dry, M. E., du Plessis, J. A. K., and Leuteritz, G. M., *J. Catal.* **6,** 194 (1966).
39. Malinowski, S., Szczepanska, S., and Sloczynski, J., *J. Catal.* **7,** 67 (1967).
40. Gregg, S. J., and Ramsay, J. D., *J. Chem. Soc. (A),* 2784 (1970).
41. Mustard, D. G., and Bartholomew, C. H., *J. Catal.* **67,** 186 (1981).
42. Smith, J. S., Thrower, P. A., and Vannice, M. A., *J. Catal.* **68,** 270 (1981).
43. Walker, P. L., Jr., Shelef, M., and Anderson, R. A., "Catalysis of Carbon Gasification," in "Chemistry and Physics of Carbon" (P. L. Walker, Jr., Ed.), Vol. 4, p. 287. Dekker, New York, 1968.
44. McKee, D. W., *in* "Chemistry and Physics of Carbon" (P. L. Walker, Jr. and P. A. Thrower, Eds.), Vol. 16, p. 1. Dekker, New York, 1981.
45. Wen, W. Y., *Catal. Rev.-Sci. Eng.* **22**(1), 1 (1980).
46. Wigmans, T., and Moulijn, J. A., *in* "Proceedings, 7th Int. Congress on Catalysis, Tokyo, 1980," p. 501. Kodansha, Tokyo, 1981.
47. Wigmans, T., Elfring, M., Hoogland, A., and Moulijn, J. A., *in* "Proceedings, Int. Conference on Coal Science, Düsseldorf, September 1981," p. 301. Verlag Glückauf GmbH, Essen, 1981.
48. Cabrera, A. L., Heinemann, H., and Somorjai, G. A., *Chem. Phys. Lett.* **81,** 402 (1981).
49. Cabrera, A. L., Heinemann, H., and Somorjai, G. A., *J. Catal.* **75,** 7 (1982).
50. Holstein, W. L., and Boudart, M., *J. Catal.* **75,** 337 (1982).
51. Rao, Y. K., Adjorlolo, A., and Haberman, J. H., *Carbon* **20,** 207 (1982).
52. "Proceedings, Int. Symposium Fundamentals of Catalytic Coal and Carbon Gasification." Amsterdam, The Netherlands, September 1982.
53. Soni, Y., and Thomson, W. J., *Ind. Eng. Chem. Process Des. Dev.* **18,** 661 (1979).
54. Carberry, J. J., Kuczynski, G. C., and Martínez, E., *J. Catal.* **26,** 247 (1972).
55. Rao, M., M. S. paper, The Pennsylvania State University, 1982.
56. Levy, R. B., and Boudart, M., *J. Catal.* **32,** 304 (1974).
57. Walker, P. L., Jr., Vastola, F. J., and Hart, P. J., *in* "Fundamentals of Gas–Surface Interactions" (H. Saltsburg, J. N. Smith, Jr., and M. Rogers, Eds.), p. 307. Academic Press, New York, 1967.
58. Feates, F. S., Harris, P. S., and Reuben, B. G., *J. Chem. Soc. Faraday Trans. I* **70,** 2011 (1974).